The EUMETSAT Network of Satellite Application Facilities

NWP SAF
Numerical Weather Prediction

Associate Scientist mission report

Mission no. AS09-04

Document NWPSAF-MO-VS-042

Version 1.0

2 June 2010

The RTTOV UWiremis IR land surface emissivity module

Eva E. Borbas[1] and Benjamin C. Ruston[2]

[1]Space Science and Engineering Center, University of Wisconsin, Madison, WI, USA

[2]Naval Research Laboratory, Monterey, Ca, USA

Met Office ECMWF KNMI METEO FRANCE Toujours un temps d'avance

The RTTOV UWiremis IR land surface emissivity module

Eva E. Borbas[1] and Benjamin C. Ruston[2]

[1]Space Science and Engineering Center, University of Wisconsin, Madison, WI, USA

[2]Naval Research Laboratory, Monterey, Ca, USA

This documentation was developed within the context of the EUMETSAT Satellite Application Facility on Numerical Weather Prediction (NWP SAF), under the Cooperation Agreement dated 1 December, 2006, between EUMETSAT and the Met Office, UK, by one or more partners within the NWP SAF. The partners in the NWP SAF are the Met Office, ECMWF, KNMI and Météo France.

Change record			
Version	Date	Author / changed by	Remarks
0.1	28.5.10	E. Borbas, B. Ruston	Initial draft
0.2	2.6.10	R Saunders	Comments on draft
1.0	2.6.10	E. Borbas, B. Ruston	Revised to address comments. Version for release.

Table of Contents

Scope **3**

1. Introduction **3**

2. UW Infrared High Spectral Resolution (HSR) Emissivity Algorithm Description **4**

3. The modified UW global IR land Surface Emissivity database **6**

Year/Version selection *6*

4. Emissivity over snow and sea-ice **8**

5. The variances of the UW IR global land surface emissivity **10**

6. Impact of emissivity on calculated IR brightness temperatures **11**

Evaluation of the RTTOV UWiremis module with SEVIRI data *12*

Evaluation of the RTTOV UWiremis module with IASI data *14*

7. Test of the RTTOV UWiremis module in assimilation mode **16**

8. Conclusions and future plans **23**

9. References **24**

Scope

This document describes the scientific approach to a study that was performed by Principal Investigator Dr. Eva Borbas at the University of Wisconsin-Madison Space Science and Engineering Center (UW-SSEC) under contract to the EUMETSAT NWP-SAF between January 1 2009 and September 30 2009. The objective of this study was to provide emissivity and an estimated mean and variance of infrared land surface emissivity at high spectral resolution (HSR) for input to RTTOV (v10 and later). The RTTOV fast radiative transfer model is a key NWP-SAF deliverable used in simulating the Earth emitted radiance at the top of the atmosphere as observed by operational weather satellites. Providing improved techniques for simulating infrared radiances over land using RTTOV is an important goal. The existing calculations of upwelling infrared radiances over land with RTTOV v9 are reliant on a single emissivity value, assumed to be a constant of 0.98 for all wavelengths. Recently an infrared emissivity atlas **(**http://cimss.ssec.wisc.edu/iremis) and high spectral resolution emissivity algorithm based on MODIS and laboratory measurements have been developed by Seemann et al. (2008) and Borbas et al. (2007). They have been shown to provide more accurate simulations of SEVIRI radiances (M. König, pers comm., and Koenig and de Coning [2009]) over land. The objective of this project is to provide a simple user interface which can be used with RTTOV (v10 onwards) and provide emissivity estimates for input to RTTOV and their associated error covariance for data assimilation applications. In this document, the theory of the new IR land surface emissivity module (called RTTOV UWiremis module), its evaluation with SEVIRI and IASI observations and its assessment in assimilation mode will be shown.

1. Introduction

An accurate infrared land surface emissivity product is critical for deriving accurate land surface temperatures, needed in studies of surface energy and water balance. An emissivity product is also useful for mapping geologic and land-cover features. Current sensors provide only limited information useful for deriving surface emissivity and researchers are required to use emissivity surrogates such as land-cover type or vegetation index in making rough estimates of emissivity. Inaccuracies in the emissivity assignment can have a significant effect on atmospheric temperature and moisture retrievals. To accurately retrieve atmospheric parameters from IR sounders, a global database of land surface emissivity with broad spectral coverage and fine spectral resolution is required. An accurate emissivity is also required for any application involving calculations of brightness temperatures such as the assimilation of radiances into weather models or simulation studies for future instrument design and preparation.

The Cooperative Institute of Meteorological Satellite Studies (CIMSS) at the University of Wisconsin (UW) has recently developed an algorithm that provides high spectral resolution (HSR) IR land surface emissivity from 3.6 to 14.3 μm using as input from a monthly composite database defined globally at 0.05-degree spatial resolution. The HSR IR emissivity spectrum is derived using an eigenfunction representation of high spectral resolution laboratory measurements of selected materials applied to the UW/CIMSS

Baseline Fit (BF) global infrared land surface emissivity database (Seemann et al, 2008). An interface to the UW HSR emissivity algorithm with the UW BF emissivity database has been implemented for the RTTOV model. The implementation, testing, and evaluation of that HSR emissivity module is described in the remainder of this document. The sections below describe the UW IR Emissivity algorithm, the methods used to create a custom UW global IR land surface emissivity database specifically for this project, the approach taken for snow and sea-ice emissivity surfaces, a newly developed spatial variance product, an evaluation of the RTTOV software module by forward radiance comparison with satellite observations from METOP-A and METEOSAT, a preliminary evaluation of the RTTOV module in a NWP data assimilation scheme, and an overall summary of the project.

2. UW Infrared High Spectral Resolution (HSR) Emissivity Algorithm Description

Significant progress has been made during the past decade in the measurement of infrared land surface emissivity from space. In particular, the NASA EOS program has contributed to observing land surface emission at a range of spatial, temporal, and spectral scales with the ASTER, MODIS, and AIRS sensors. However, even with this wealth of new observations there is a need to fill in the gaps in the spectral and spatial coverage of the derived emissivity measurements to support new operational sounders and imagers such as IASI on METOP and SEVIRI on METEOSAT. The approach for taking advantage of selected window channel measurements of infrared emissivity from the MODIS sensor and extending that to a continuous coverage of the thermal infrared at low spectral resolution is described in Seeman et al. (2008) so those details will not be repeated here. The advantage of the approach described in Seeman et al. (2008) is that an emissivity value is provided at all wavelengths, in particular for the "sounding" channels for which a portion of the radiance emitted from the surface is transmitted through the atmosphere to the satellite sensor. Seeman et al. (2008) provides an example of the need for accurate emissivity in infrared sounding channels to derive total column water vapor. The low spectral resolution, but moderate spatial resolution product described in Seeman et al (2008) is called the UW/CIMSS Baseline Fit (BF) global infrared land surface emissivity database. The low spectral resolution of the UW BF database is adequate for filter radiometers but is not sufficient to capture the detailed spectral structure of the surface emissivity which affects the radiances observed by the advanced IR sounders (AIRS, IASI, and CrIS). The approach developed at the University of Wisconsin to derive high spectral resolution (HSR) infrared emissivity measurements from measurements made at selected wavelengths is known as the UW HSR algorithm.

The UW HSR algorithm takes advantage of a wide variety of laboratory measurements of terrestrial materials (minerals, soils, vegetation, fresh water, salt water, snow, ice, etc.) which have been made at high spectral resolution for a continuous range of the infrared (Salisbury et al., 1992, 1994). The laboratory measurements have the advantage of being performed using short path lengths and under purged conditions so that the effects of water vapor absorption (and other gases) can be minimized. They can also take advantage of laboratory spectrometers which have resolving powers of 1000 or more. The laboratory measurements used in the derivation of the emissivity in this paper were drawn from the

MODIS emissivity library (http://www.icess.ucsb.edu/modis/EMIS/html/em.html) and the ASTER spectral library (Salisbury et al. 1994). Figure 1 shows the laboratory spectra selected for use in this HSR study.

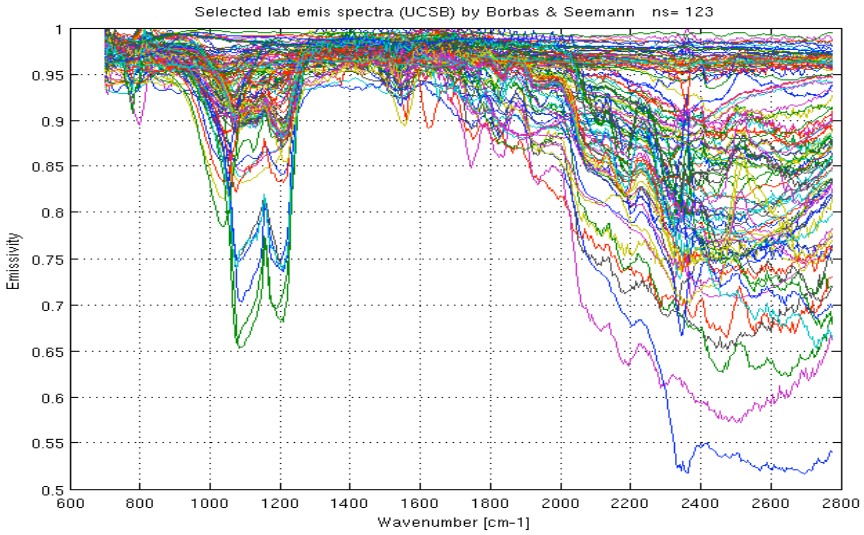

Figure 1: Selected laboratory spectra (in different colors) used in the HSR algorithm study.

The first Principal Components (PCs or eigenvectors) of 123 selected laboratory spectra with wavenumber resolution between 2 to 4 cm^{-1}, at 416 wavenumbers were regressed against the 10 hinge points (3.6, 4.3, 5.0, 5.8, 7.6, 8.3, 9.3, 10.8, 12.1, and 14.3 μm) of the UW/CIMSS BF emissivity as follows:

$$\vec{\mathbf{e}} = \vec{\mathbf{c}}\mathbf{U}$$

where $\vec{\mathbf{e}}$ is the lab spectra on the 10 hinge points, $\vec{\mathbf{c}}$ is the PCA coefficient vector and $\mathbf{U}$ is the matrix of the first PCs of the lab emissivity spectra on the reduced spectral resolution. After calculating the coefficients ($\vec{\mathbf{c}}$), the high spectral resolution emissivity values are determined at the same latitude and longitude point given in the BF input data.

The accuracy of the new HSR emissivity data is dependent upon the accuracy of the input UW BF emissivity data and hence the MODIS monthly MYD11 measurements. The BF approach uses a conceptual model of the spectral shapes observed in laboratory measurements of emissivity to derive baseline spectra, and then incorporates MODIS MYD11 measurements (at six wavelengths: 3.8, 3.9, 4.0, 8.6, 11, and 12 μm) to adjust the emissivity at 10 hinge points (see Seemann et al., 2008 for more details). The MYD11 products are derived by the MODIS day/night Land Surface Temperature (LST) algorithm (Wan and Li, 1997, Wan et al. 2004) that retrieves Ts-day, Ts-night, and band emissivities simultaneously with the range of viewing zenith angle separated into 16 sub-ranges in the range of 0-65 degrees.

In the PCA regression method described above, only about six eigenfunctions are required to represent the variations within the laboratory dataset with good accuracy. The maximum number of PCs allowed is 10 which matches the number of spectral points contained in the input BF emissivities. It has been found that using too many PCs can lead to an unstable

solution. Previously tests were performed to determine the number of PCs to use (see details in Borbas et al. 2007. From these tests we have determined the optimal number of PCs is 6, which was used in this study.

3. The modified UW global IR land Surface Emissivity database

The monthly, so-called UW/CIMSS Baseline Fit (BF) global infrared land surface emissivity database has been developed and available since 2006 at the http://cimss.ssec.wisc.edu/iremis/ website and includes data from January 2003 till December 2009 (at present) at ten wavelengths (3.6, 4.3, 5.0, 5.8, 7.6, 8.3, 9.3, 10.8, 12.1, and 14.3 microns) with 0.05 degree spatial resolution. To reduce the memory necessary for loading the data into the RTTOV, the original database has been reduced to 0.1-degree spatial resolution and a simple land/sea mask has been applied for storing only the land data. The emissivity flag in the original database has been modified accordingly. Additionally, artificially low emissivity values have been found by Andrew Collard (2009, sec 2.2) over the coastlines. Hence a more conservative emissivity flag has been introduced to be able to select the high confidence data for users who need it. In the new flag more information about water contamination and coastlines are added. The inland water or coastline contaminated pixels were indentified by applying the official MODIS (MOD44) land/sea mask. The definition of the emissivity flag values is described in the RTTOV UWiremis Technical Document (RTTOV UWIR TD, 2010). Figure 2 shows the original and modified, new emissivity flag, and the MODIS land/sea mask and land fraction, which were used to determine the new flag values. An application of using the emissivity flag for filtering the data for August 2007 is demonstrated in Figure 3. As you can see, the lower values represent the more conservative filtering.

Year/Version selection

Because the BF emissivity data uses the MODIS MYD11 product as input, BF emissivity values are affected by changes in the MYD11 algorithm. The official MODIS products have been reprocessed at the NASA LP DAAC a number of times. The current collection (version) is 5, however significant differences were found between MYD11 collection 4 and 5 data (especially over desert areas). Due to these differences beginning in 2007 the NASA LP DAAC decided to continue to produce collection 4 data beyond December 2006 but using only the available collection 5 MODIS input data like cloud mask, L1B data and atmospheric profiles. The new version of MYD11 data is called collection 4.1. You can find more information about the MYD11 collection 041 product in the following document: http://landweb.nascom.nasa.gov/QA_WWW/forPage/C41_LST.doc. As a result the UW BF emissivity database is based on MODIS MYD11 Collection 4 data between 2003 and 2006 and on the MYD11 Collection 4.1 data beyond December 2006. Since there might be differences in the MODIS collections due to the cloud mask, L1B and profile data, over certain areas it is not recommended to use the BF database as a continuous dataset. After some tests (see Collard, 2009) , the twelve months of 2007, (derived from MYD11 collection 4.1 product) were chosen for implementing into the RTTOV UWiremis module.

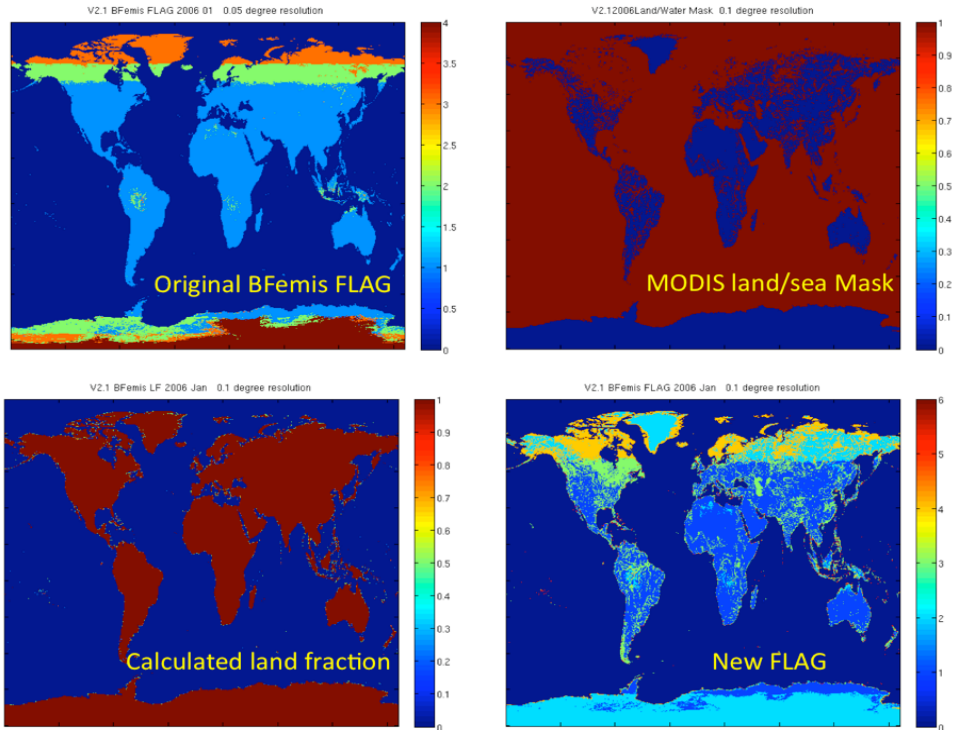

Figure 2: (top left) The emissivity flag in the original BF emissivity database for January 2007; (top right) the MODIS (MOD44) land/sea mask; (bottom left) the calculated land fraction from the spatial reduction; (bottom right): the new emissivity flag used in the RTTOV UWiremis module.

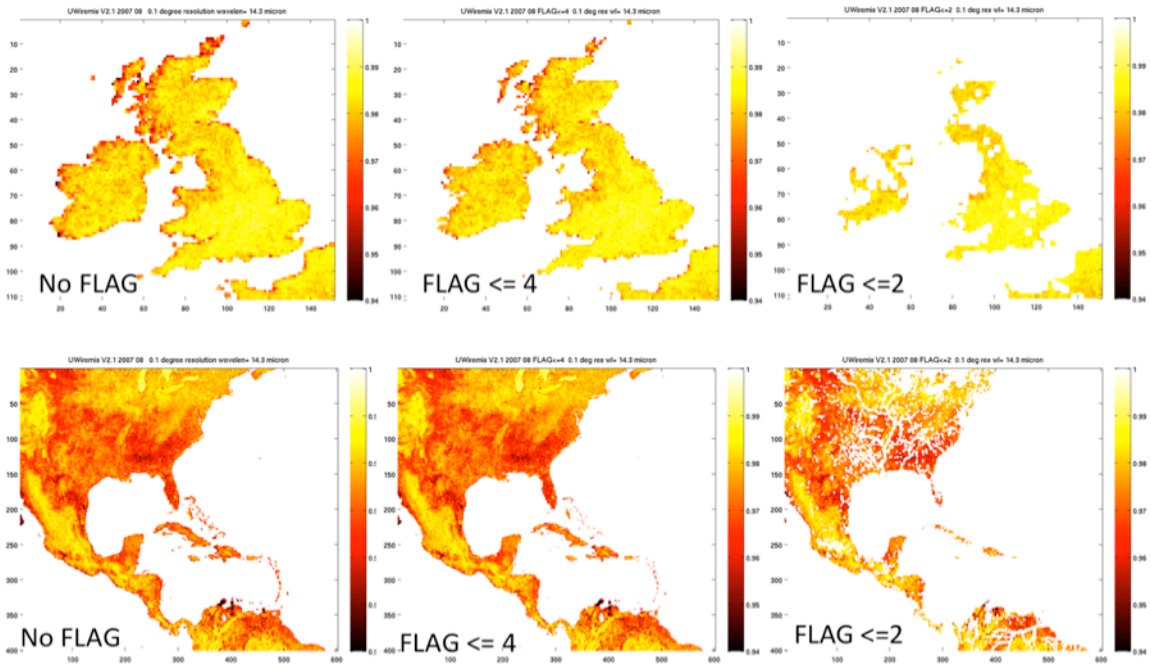

Figure 3: Applying the flag for filtering out the water contaminated pixels over the British Isles (top) and the Caribbean region (bottom) on August 2007 (MYD11 C041) at 14.3 μm.

4. Emissivity over snow and sea-ice

The UW BF emissivity database is a monthly mean emissivity database, which does not necessarily reflect the actual snow or sea ice coverage. To be able to take into account this information, the mean and standard deviation of snow and sea-ice emissivity spectra is added to the module (see Figure 4). The emissivity values for snow and sea-ice data come from a near-real time 1D-Var emissivity retrieval performed at NRL from July 2006 – January 2008 (Ruston et al., 2008). This retrieval was performed with the HIRS-3 and -4 sensors and used the Johns Hopkins University (JHU) spectral library within the ASTER spectral library to interpolate to all wavenumbers. To be able to apply the snow emissivity spectra, the snow fraction was added to the RTTOV profile structure. If this value is larger than 0, the emissivity is a linearly blend average of snow and land emissivity values. The standard deviations for snow and sea-ice are estimated from the global snow and sea-ice values. Because of the large uncertainty in the effective surface emitting temperature in the 1D-Var, the estimates of the standard deviation of 0.005-0.01 were inflated to 0.015 for the conservative global estimate.

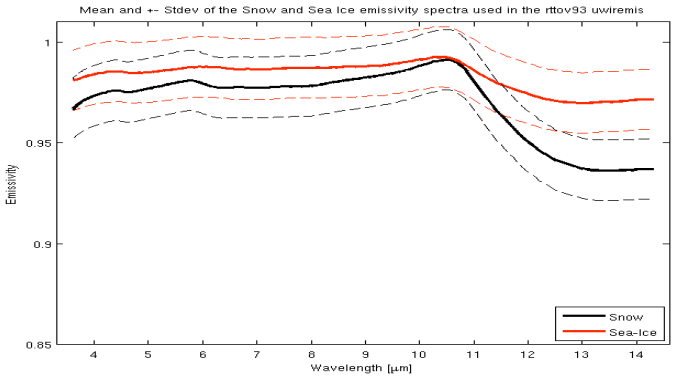

Figure 4: The mean and the mean ± standard deviation of the snow and sea-ice emissivity spectra added to the RTTOV UWiremis module.

Figure 5 shows the snow fraction map and the affected brightness temperature differences at three selected wavelengths on January 15, 2008 at 1200UTC. Over two selected locations brightness temperature differences up to 2K are shown at higher snow fraction (cover) in Figure 6 (bottom). The top panels illustrate how the linearly band average between the snow and land emissivity (no snow) works: at 100% snow cover the emissivity spectra passed out of RTTOV matches the snow spectra in the RTTOV module, while the emissivity spectra with 65 % snow cover is located between the 100 and 0 % snow cover spectra. In Figure 7 the latitudinal cross section of brightness temperature differences shows how the snow cover corresponds to the deviations between snow covered and snow free input.

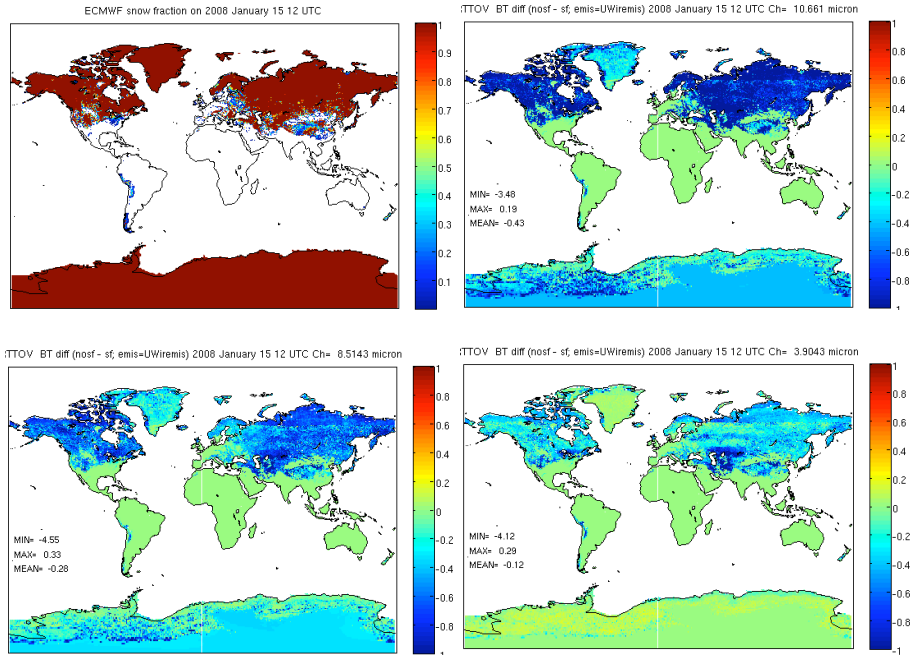

Figure 5: (left) Snow fraction map (top left, white stands for zero) and calculated brightness temperature differences (no snow fraction – snow fraction) at 10.8 (top right), 8.5 (bottom left) and 3.9 (bottom right) μm on January 15, 2008, 1200 UTC. UWiremis is used in the forward calculation. The minimum, maximum and mean of the differences are also added to the figures.

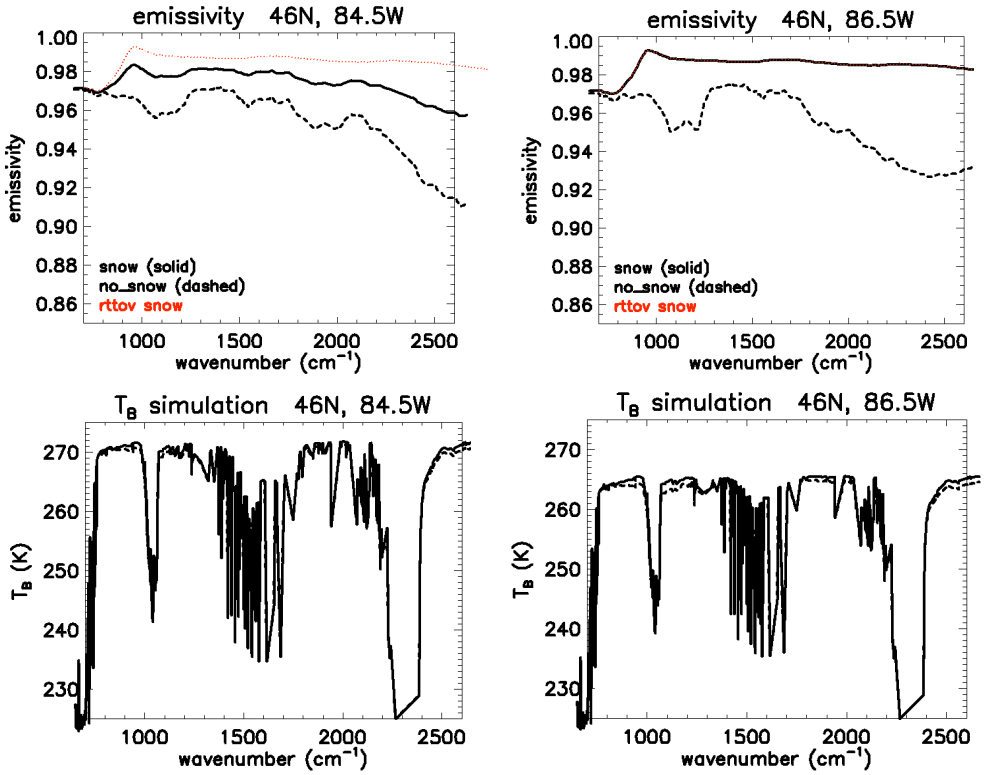

Figure 6: Emissivity spectra (top) and IASI simulated brightness temperatures (bottom) of two selected locations applying snow fraction of 0.65 (left) and 1.0 (right) on January 15, 2008.

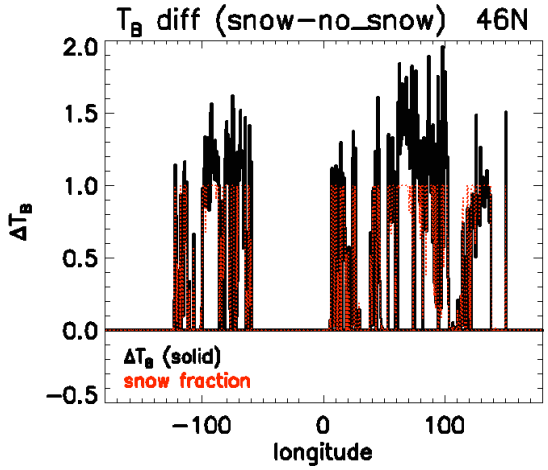

Figure 7: Latitudinal cross section of brightness temperature differences between using the snow fraction as input or not (Lat:46N for 10.6μm). Snow fraction varies between 0 and 1. High snow fraction causes large T_B differences; no snow cover results in no T_B difference.

5. The variances of the UW IR global land surface emissivity

A spatial variance estimate of the UWiremis database has been created for each month on a 0.5x0.5 degree grid on the full 416 spectral resolutions. The 0.5-degree resolution has been chosen to avoid memory load issues. The mean and the variance of the covariance matrix from 100 points of the original 0.05-degree resolution UWiremis dataset between year 2003 and 2006 were calculated, which resulted in 400 observation points for one grid. No threshold for the number of observations was applied and no interchannel correlations have been included in this release. The data files include this information for user application. Figure 8 illustrates the standard deviation of the UWiremis database at 8.6 and 4 μm for August between 2003 and 2006. The areas with high variation correlate with the less or non-vegetated areas. The error estimation (mean and variance) of sea-ice and snow emissivity spectra is also included in the RTTOV UWiremis module. Due to the large uncertainty in the effective surface emitting temperature, standard deviations of the snow and sea-ice emissivity are conservatively set to 0.015 as a global estimate. The ocean emissivities use the ISEM model; the uncertainty of the ocean IR emissivity raises with wind speed (particularly when >10 m/s) and has a temperature dependence greatest at 800 cm^{-1} and at 3000 cm^{-1}. A conservative estimate of 0.01 is used as a global estimate and further revisions should be able to reduce the uncertainty estimates when wind speed is low and in a wavenumber region with low variability.

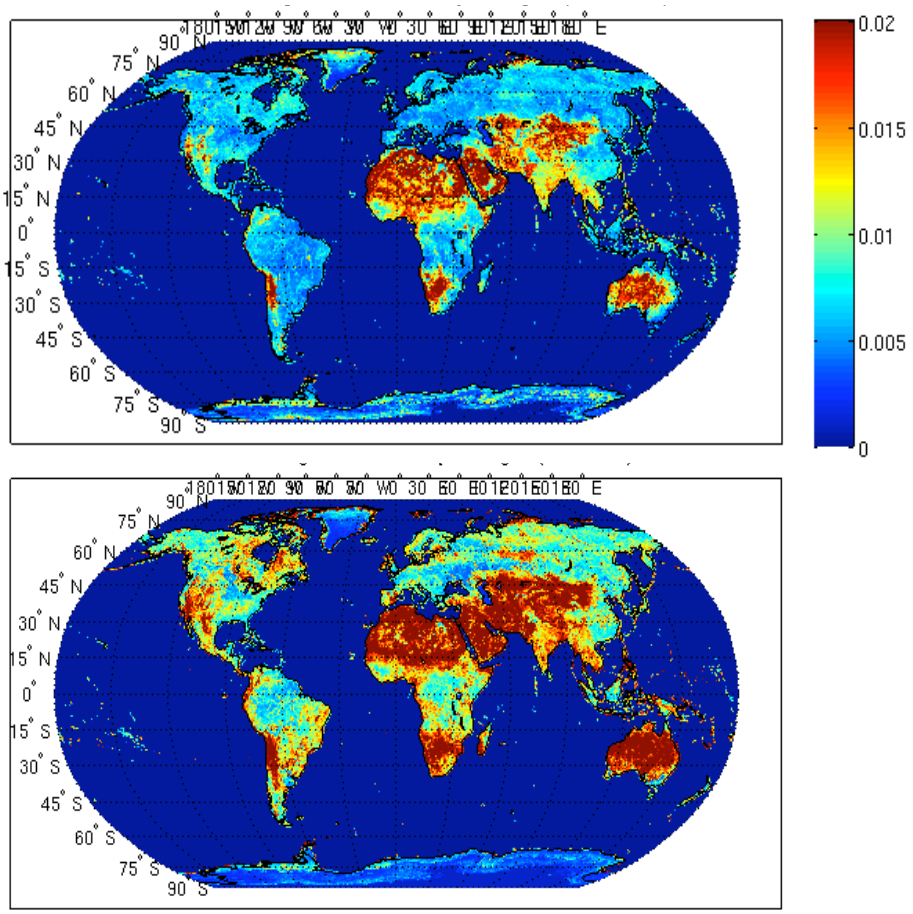

Figure 8: Standard deviation of the UWiremis HSR emissivity database at 8.6 (top) and 4 (bottom) μm for August between 2003 and 2006.

6. Impact of emissivity on calculated IR brightness temperatures

For the evaluation of the RTTOV UWiremis module, SEVIRI and IASI data have been chosen: SEVIRI represents a broadband instrument on a geostationary satellite (Meteosat Second Generation (MSG)) and IASI represents a high spectral resolution IR instrument on a polar orbiting satellite (METOP-A). Brightness temperatures were calculated for these two instruments using the RTTOV default emissivity value (0.98) and the new RTTOV UWiremis module for four selected global days representing each season: Jan 15, Apr 14, July 15 and Sept 29 2008. These two sets of simulated BTs then were compared to the collocated observed BTs over land pixels (excluding coastlines) and clear sky conditions only. The following simplifications were applied during the calculations: the satellite, the sun zenith and azimuth angles were set to 0 degrees; snow fraction was not applied; and no other trace gases were added besides water vapor. To determine the clear conditions, the MAIA cloud mask was applied for both instruments. The comparisons were further subdivided by day and night using the threshold of 90 degrees for the observed solar azimuth angle. The ECMWF 6 hour reanalyses fields at 0.5-degree spatial resolution were chosen for the

forward calculations. To make the collocation, 2 hour and 30 min time gaps were allowed for night and day respectively for the IASI instrument. For SEVIRI, only the data at the ECMWF analyses time were used. For spatial collocations, the calculated BTs at the ECMWF grid points were bilinearly-interpolated to the center of the IASI or SEVIRI FOVs.

Evaluation of the RTTOV UWiremis module with SEVIRI data

SEVIRI brightness temperatures were calculated for the 8 IR SEVIRI channels with the central wavelength: 3.9, 6.2. 7.4, 8.7, 9.7, 10.7, 12.0 13.3 μm. Observations less than 60 degrees of satellite zenith angles were used in this study.

As an example, Figure 9 and 10 show the mean differences (bias) between the calculated and observed BTs for July 15, 2008 separated by day and night. Figure 9 illustrates the results over the whole observation area and Figure 10 is over the subset of Sahara Desert. On the top panels, the black lines represent the bias when the calculation was made with the RTTOV default value (0.98) and the red lines represent the bias when the calculations were made with the RTTOV UWiremis module. The bottom panels on the figures show the differences between the black and red curves. The positive values mean positive effect (or reduced bias) by using the new UWiremis module. Over the whole observed area the bias was most reduced at the 4 and 8.7 μm channels by 1.5 and 3.5 K respectively and these values were increased to 3.5 and 8 K over the Sahara desert region (see Figure 10, bottom panels).

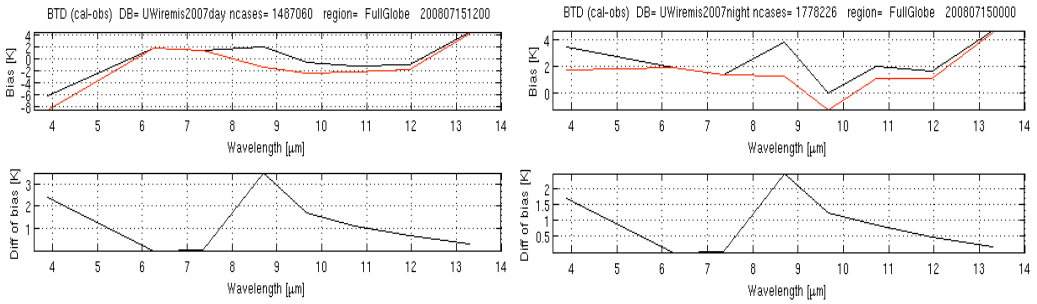

Figure 9: Biases of SEVIRI brightness temperatures (calc-obs) for July 15, 2008 when RTTOV default (black) and RTTOV UWiremis module (red) were used in the calculation (top panels). The statistics were calculated over the full area (shown right), but separated by day (left panels) and night (right panels). The default minus UWiremis biases show a consistent impact both day and night (bottom panels).

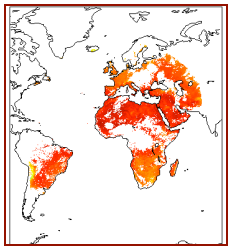

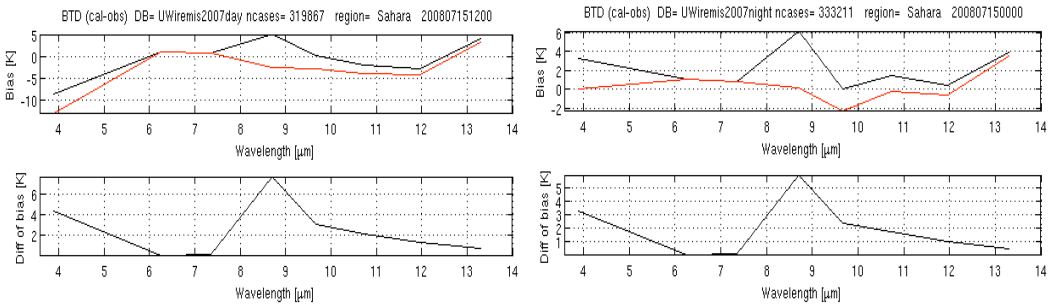

Figure 10: Same as Figure 9 except the statistics were calculated over the Sahara dessert region.

There is a systematic bias across all surface sensitive channels at daytime, which is probably due to the skin temperature differences between the actual and the ECMWF analyses. Furthermore there is an error in the shortwave region during the day caused by the uncertainty in the solar radiation component in the radiative transfer model. Besides these facts and looking at the shape of the effects over day and night (bottom panels of Figure 10), we can conclude that the effect is very similar in both cases. The time series of the BT biases are plotted in Figure 11 for the SEVIRI channels, which were sensitive to the surface emissivity. The bias reduction by using the UWiremis module is consistent over the four selected days representing the four seasons. Overall, the biggest impacts occur at the 3.9 and 8.7 μm channels.

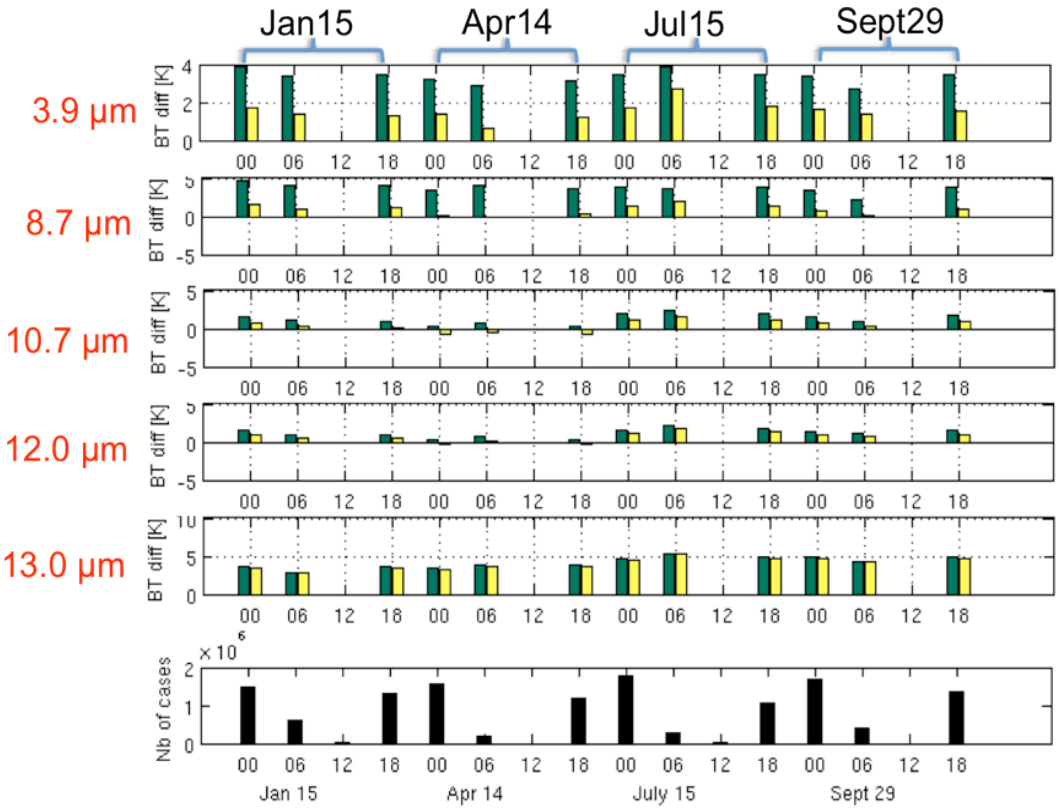

Figure 11: Time series of SEVIRI BT biases (Calc-Obs) of selected channels over the Full Area at nighttime. Yellow represents the bias when the UWiremis module was used in the calculation and

green represent bias when the RTTOV default emissivity was used in the calculation. The number of observations is also plotted on the bottom panel.

Evaluation of the RTTOV UWiremis module with IASI data

IASI brightness temperatures were calculated for 616 selected channels (NOAA/NESDIS selected subset). Collocation between IASI and ECMWF analyses are shown on Figure 12 separated by day and night for July 15, 2008 as an example. Due to the stricter, 30 minutes time limitation for daytime collocation, there was no collocation (IASI overpasses) over the Sahara during the daytime for the ECMWF Analyses times (0600, 1200 and 1800 UTC).

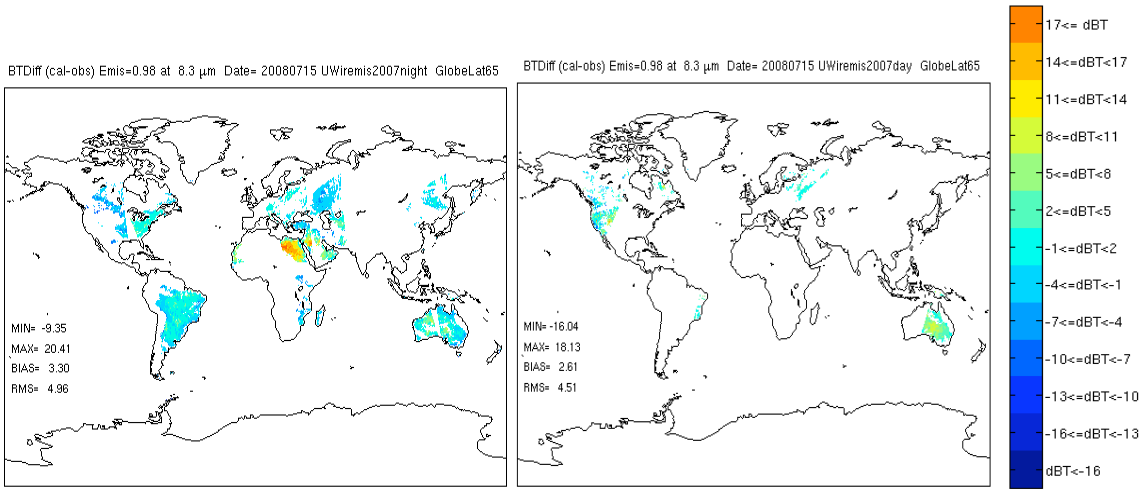

Figure 12: Brightness temperature differences (in Kelvin) for 8.3 µm between IASI observations and calculated values from ECWMF analyses using the default RTTOV emissivity, on July 15, 2008 separated by day (right) and night (left).

For the same day, similar figures to SEVIRI are shown in Figures 13 and 14. The mean differences (bias) between the calculated and observed BTs for July 15, 2008 separated by day and night over the whole globe are shown in Figure 13) and over the Sahara Desert in Figure 14. Similar to what was discussed in the previous section on the top panels, the black lines represent the bias when the calculation was made with the RTTOV default value (0.98) and red lines represent the bias when the calculations were made with the RTTOV UWiremis module. The bottom panels in the figures show the differences between the black and red curves. The positive values mean positive effect (or reduced bias) using the new UWiremis module. Over the whole globe the bias was most reduced at the 4 and 8.7 µm channels by 1.5 and 3 K respectively, and these values were increased to 5 and 12 K over the Sahara Desert region. As the bottom panel of Figure 13 indicates, the effect of using the UWiremis during the day and night is very similar (same as in the SEVIRI case).

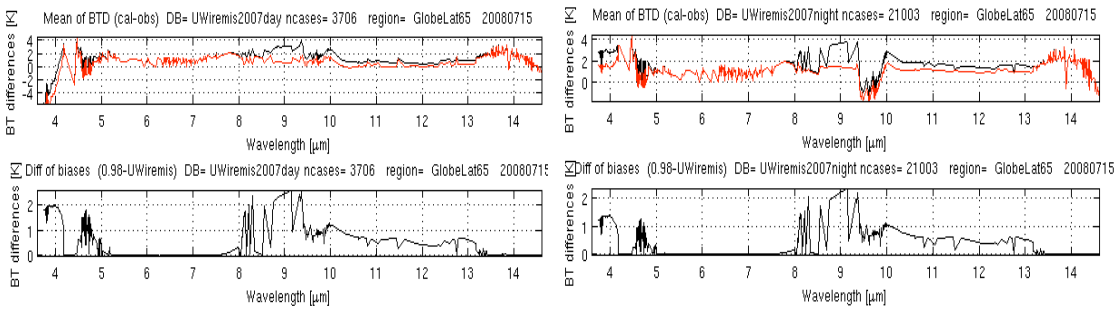

Figure 13: (top) IASI brightness temperature biases (calc-obs) for July 15, 2008 when RTTOV default (black) and RTTOV UWiremis module (red) were used in the calculations. The statistics were calculated over the whole globe (shown in Figure 11), but separated by day (left panels) and night (right panels). (bottom) The differences of the two curves in the top panels are shown. The positive values represent positive impact when the new RTTOV UWiremis module is used.

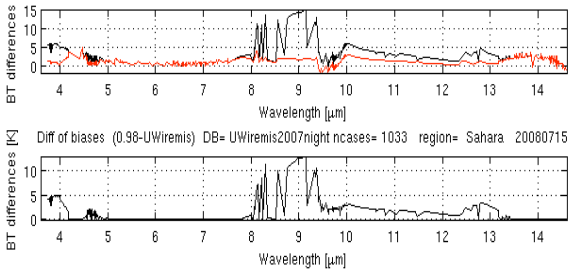

Figure 14: same as Figure 13 except the statistics were calculated over the Sahara Desert region, nighttime only.

The time series of the BT biases shown in Figure 15 for similar selected IASI channels as was shown for SEVIRI is consistent with the SEVIRI results: the bias is reduced by using the UWiremis module over the four selected days representing the four seasons. Overall, the biggest impacts occur at the 4 and 8.7-9 μm channels. Similarly to SEVIRI, negative biases occur only during the day due to the uncertainty in the solar radiation calculation and the error in the skin temperature modeling. As the bottom panel of Figure 13 indicates, the effect of using the UWiremis during day and night is very similar (same as in the SEVIRI case).

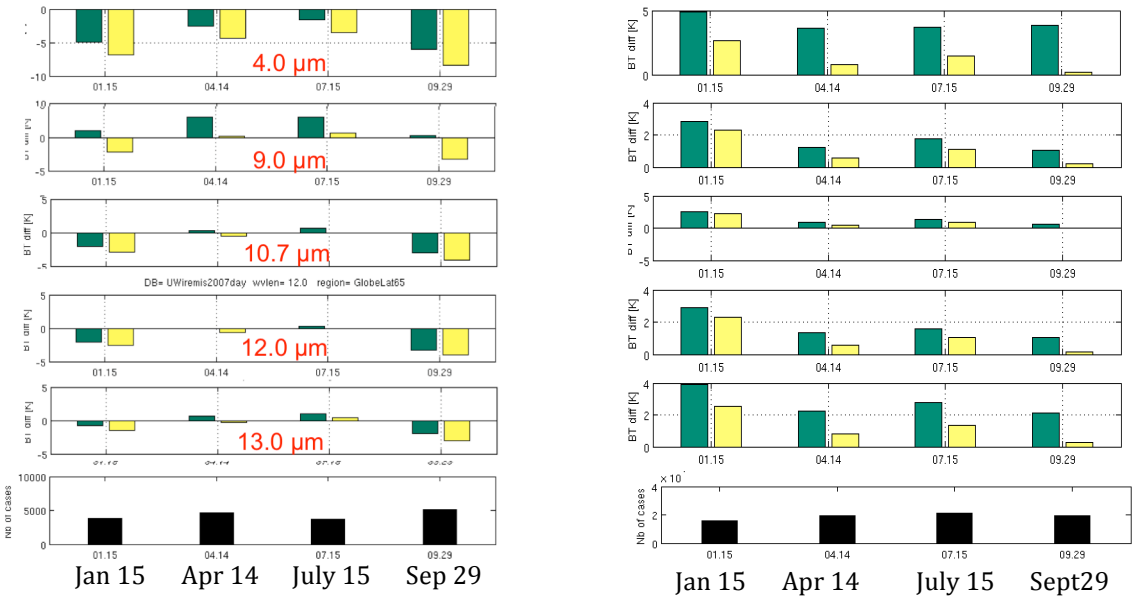

Figure 15: Time series of IASI BT biases (Calc-Obs) of selected channels over the full globe separated by daytime (left) and nighttime (right). Yellow represents the bias when the UWiremis module was used in the calculation and green represent the bias when the RTTOV default emissivity was used in the calculation. The number of observations is also plotted on the bottom panel.

7. Test of the RTTOV UWiremis module in assimilation mode

An assessment of the forecast sensitivity was performed using the NRL Atmospheric Data Assimilation System – Accelerated Representer (NAVDAS-AR) 4D-Var assimilation system. The global forecast model in NAVDAS-AR is the Navy Operational Global Atmospheric Prediction System (NOGAPS), the version used for this study has a T239 spectral resolution (equivalent to about 60km) with 42 vertical levels with its top at 0.04 hPa. A full system was run for two case study periods: 18Jan2010 – 28Feb2010, and 23Jul2009 – 31Aug2009. These studies included all conventional data including radiosondes, ship observations, and aircraft reports, GPS bending angle assimilation from COSMIC and GRAS, radiances from microwave sounders AMSUA ch3-10 and SSMIS ch2-7, and infrared sounders IASI (39 channels) and AIRS (34 channels). For both time periods two configurations were run. The first configuration is a 'base' run which contains all the above data and the IR sounders AIRS and IASI are assimilated over ocean only. The second configuration, 'uwemis,' contains all the data in the 'base' configuration with the addition of all land and sea-ice points for IR sounders derived from the UW emissivity module. In the 'uwemis' configuration an additional threshold check is performed on the (innovation * T_{skin} Jacobian) where innovation is the observed radiance minus the simulated radiance.

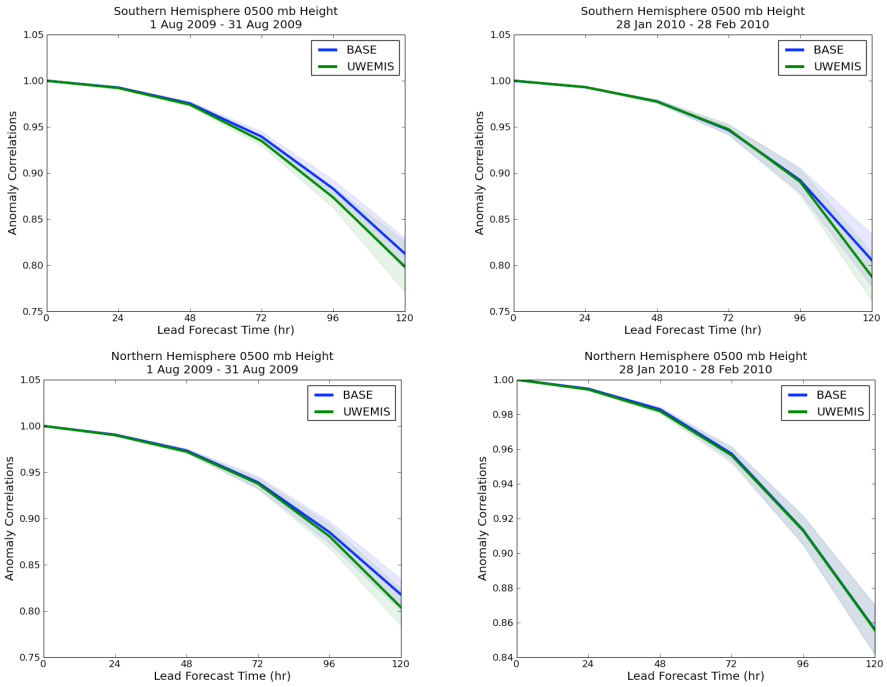

Figure 16: Shown are the Southern and Northern hemisphere 500mb height anomaly correlations with a shaded 95% confidence interval. The 'uwemis' configuration contains land points for IR sounders with emissivity from the UWemis module in RTTOV. The 'base' configuration shows the highest correlations but they are not significant at the 95% level.

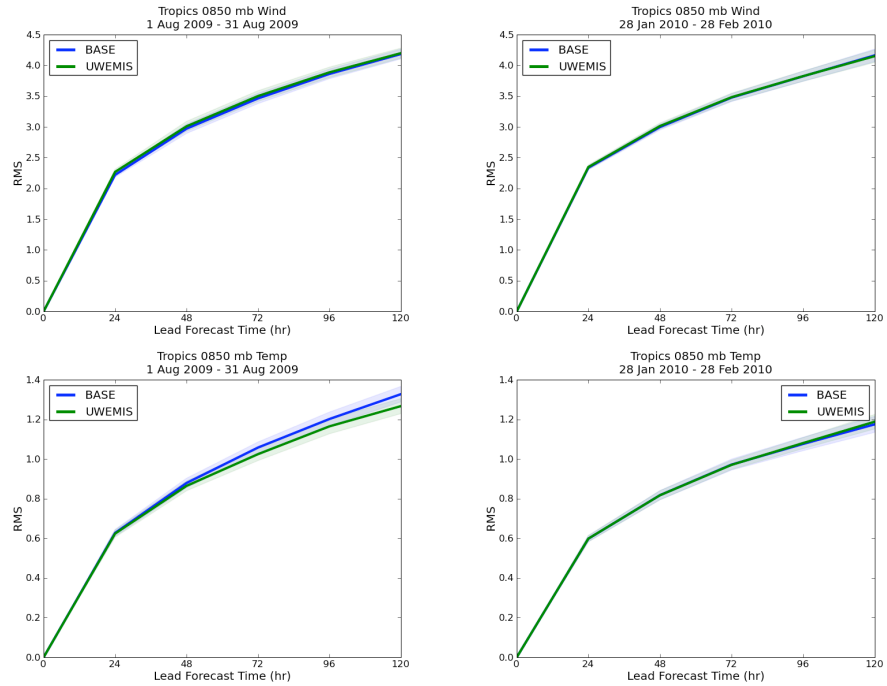

Figure 17: Shown are the 850mb vector wind RMS and temperature RMS in the Tropics with a shaded 95% confidence interval. The 'uwemis' configuration contains land points for IR sounders with emissivity from the UWemis module in RTTOV. The 'uwemis' configuration shows a reduction in the temperature RMS for Aug2009.

The self-analysis of NOGAPS is shown for the 500mb height anomaly correlation in the Southern and Northern hemispheres in Figure 16, and for the 850mb vector wind and temperature RMS for the Tropics in Figure 17. The 95% confidence interval is shaded in both cases. The 500mb anomaly correlations for the 'base' configuration performs slightly, but not significantly at 95% confidence, better than the 'uwemis' configuration. At 850mb in the tropics, the configurations seem to be performing similarly with the only outlier being the 850mb temperature RMS for the Aug2009 period, where the 'uwemis' configuration has a reduced, and qualitatively better, RMS value.

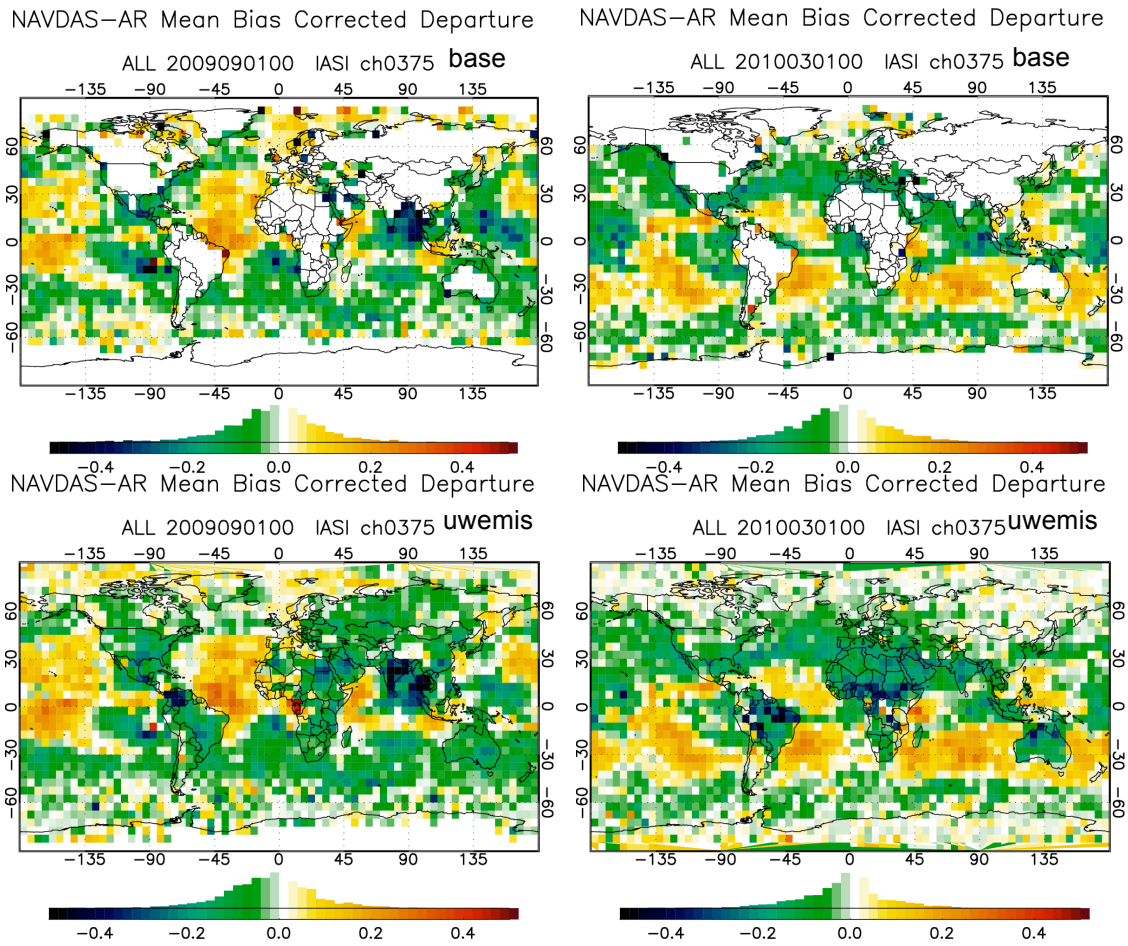

Figure 18: Mean innovations averaged for a month in 5x5 boxes for IASI channel 375 at 738.50 cm^{-1} (13.541 μm), which has a T Jacobian peak at approximately 800 hPa. The 'base' configuration is shown in the top two panels, and 'uwemis' in the bottom two.

Statistics from the innovations (observed minus simulated brightness temperature) are shown in both Figure 18 and 19. The mean bias corrected innovation is shown in 5-degree by 5-degree boxes for IASI channel 375 at 738.50 cm^{-1} (13.541 μm) which has a temperature Jacobian peak at 800hPa for the US standard atmosphere. For this lower tropospheric channel the 'uwemis' innovation histogram distribution, above the colorbar, shows no significant differences with the 'base' configuration and appears spatially coherent when passing from ocean to land. The 'uwemis' run, more noticeably in the

August 2009 case, does show greater negative innovations in the northern Indian Ocean and great positive innovations in the central tropical Pacific and tropical Atlantic ocean. This Aug2009 time period is where the temperature RMS at 850mb was lower for the 'uwemis' run, and could be tied to better atmospheric forcing by the radiances.

Figure 19 displays the time-evolution of the global standard deviation of the 6-hourly innovations for a selection of IASI channels. Time is along the x-axis, and the IASI channels are along the y-axis with assimilated channels in black. Here interestingly, a decrease in the un-bias corrected standard deviation of the innovations is seen in the 'uwemis' run, particularly for IASI channels 193-230 which are largely mid- to upper-tropospheric channels, which is a good indicator that the UWemis module in RTTOV is not negatively affecting these channels, and these channels could be included with current observation error and quality control procedures.

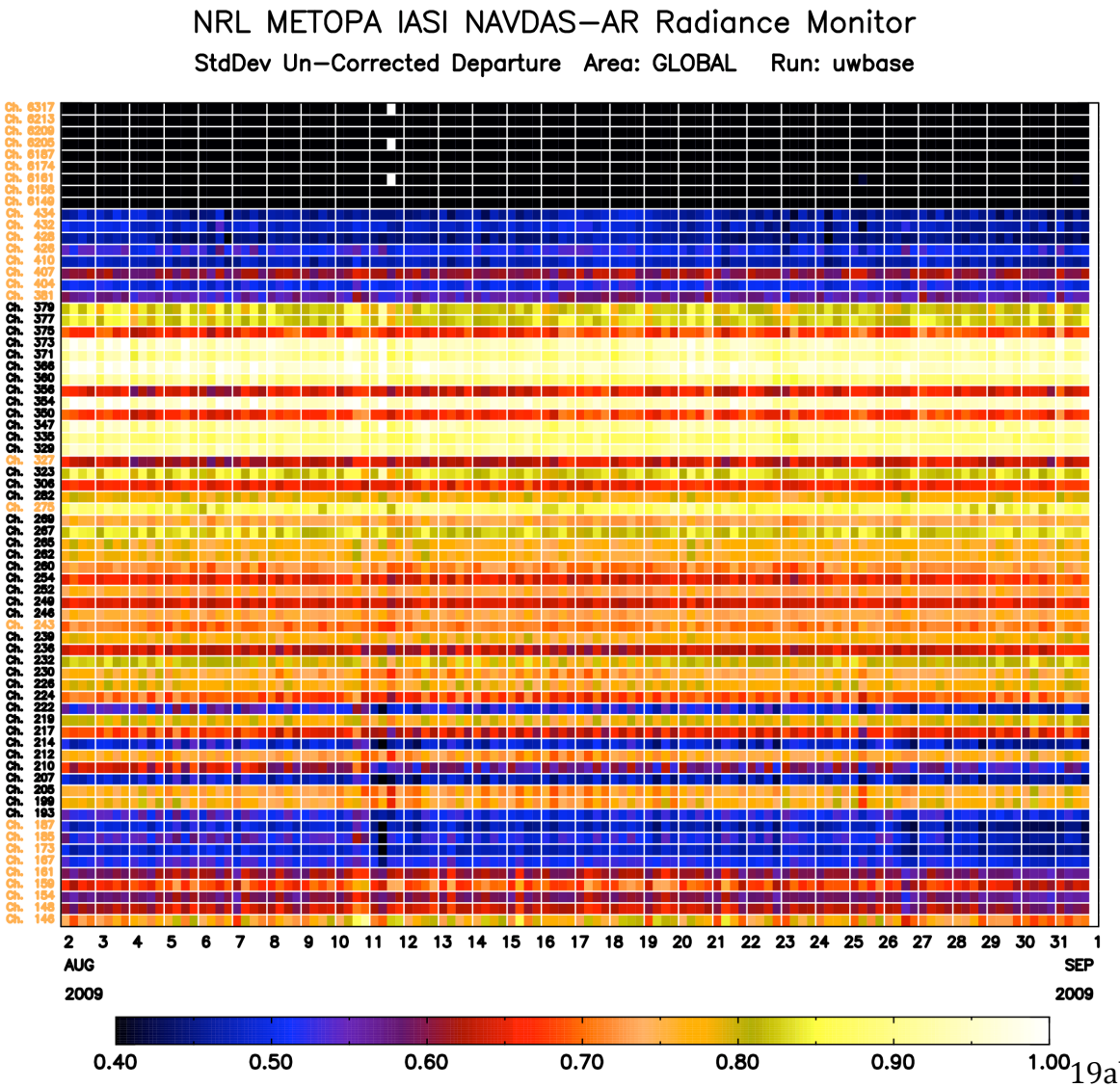

19a)

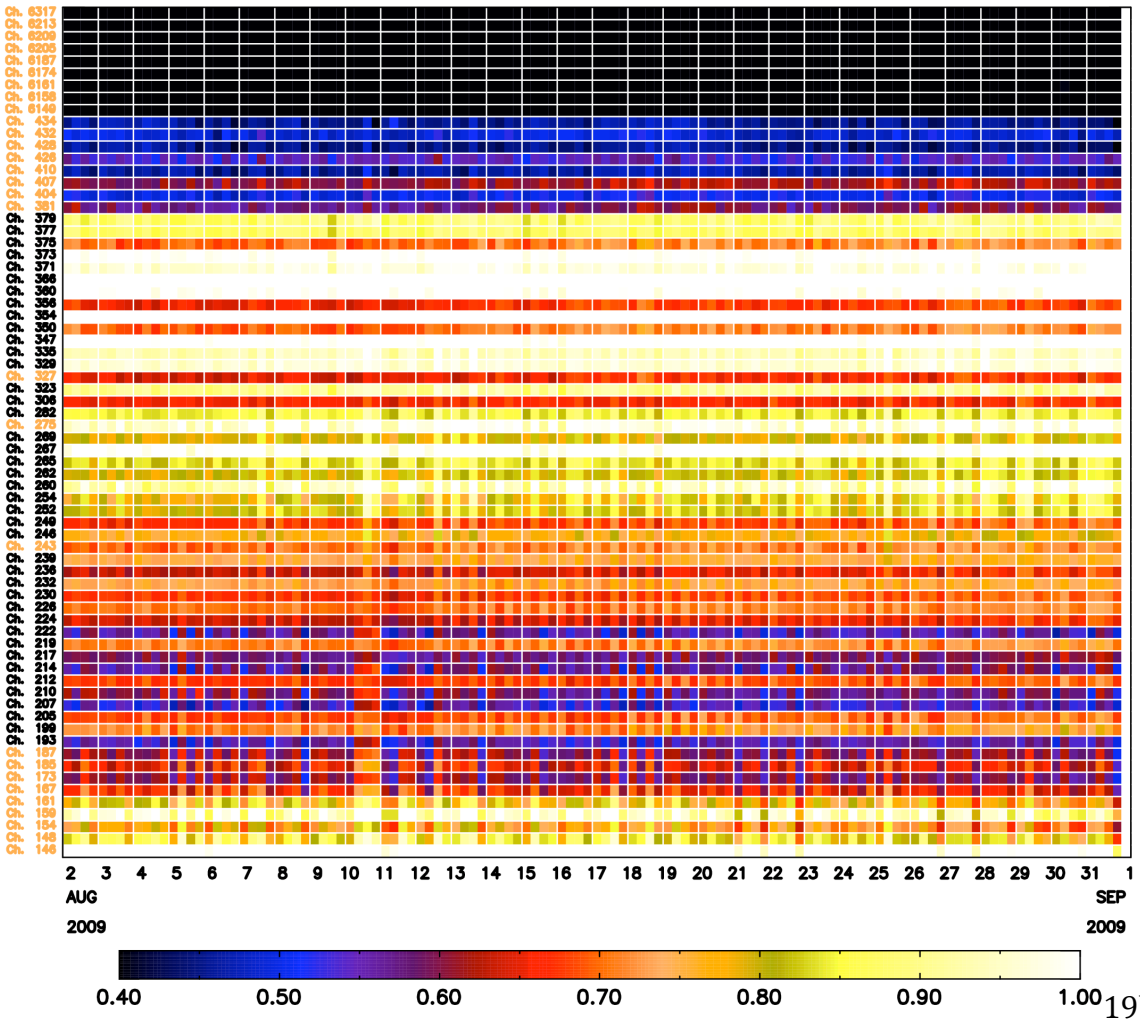
NRL METOPA IASI NAVDAS–AR Radiance Monitor
StdDev Un–Corrected Departure Area: GLOBAL Run: uwemis
2 3 4 5 6 7 8 9 10 11 12 13 14 15 16 17 18 19 20 21 22 23 24 25 26 27 28 29 30 31 1
AUG
SEP
2009
2009
0.40 0.50 0.60 0.70 0.80 0.90 1.00

19b)

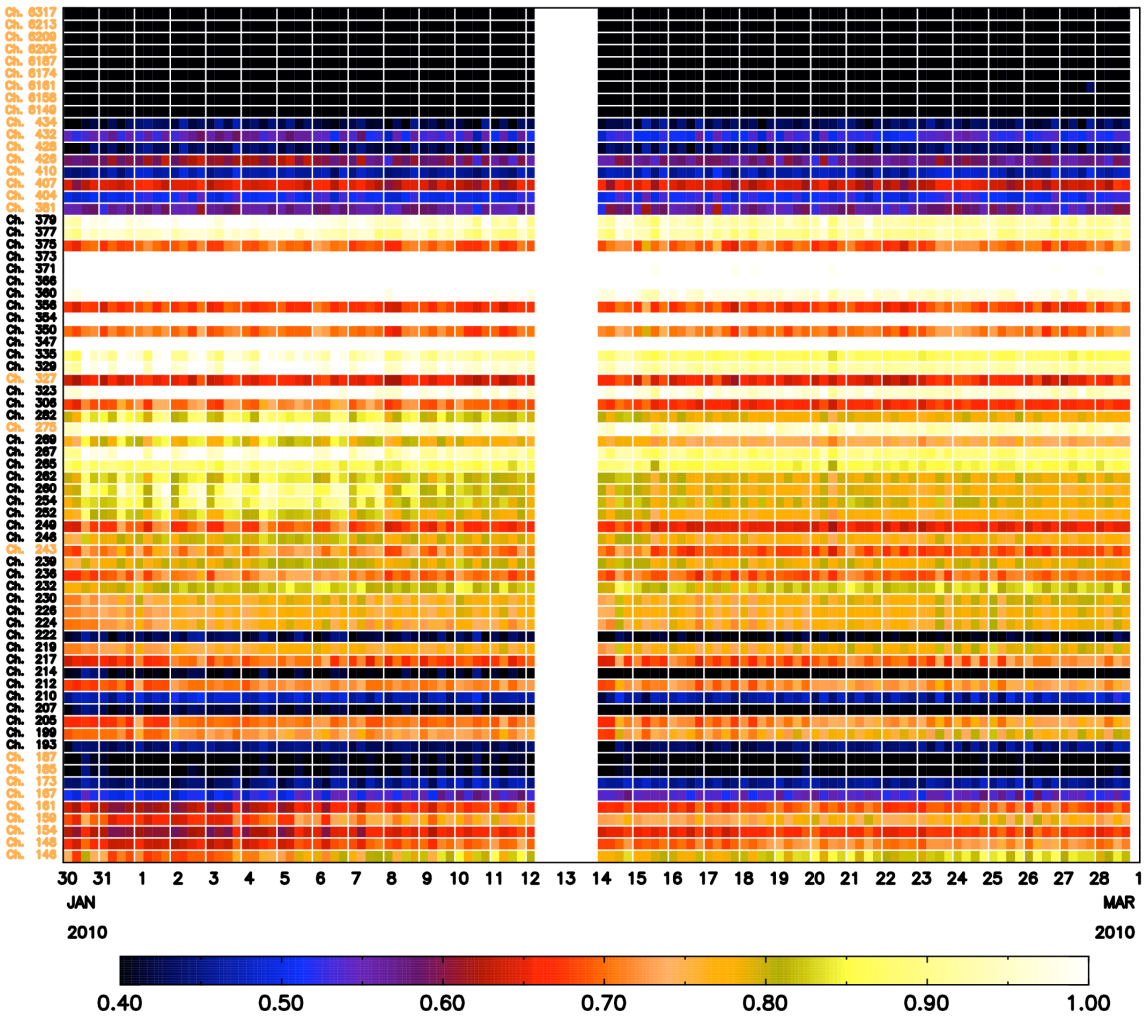
NRL METOPA IASI NAVDAS–AR Radiance Monitor
StdDev Un–Corrected Departure Area: GLOBAL Run: uwbase
30 31 1 2 3 4 5 6 7 8 9 10 11 12 13 14 15 16 17 18 19 20 21 22 23 24 25 26 27 28 1
JAN
2010
MAR
2010
0.40 0.50 0.60 0.70 0.80 0.90 1.00

19c)

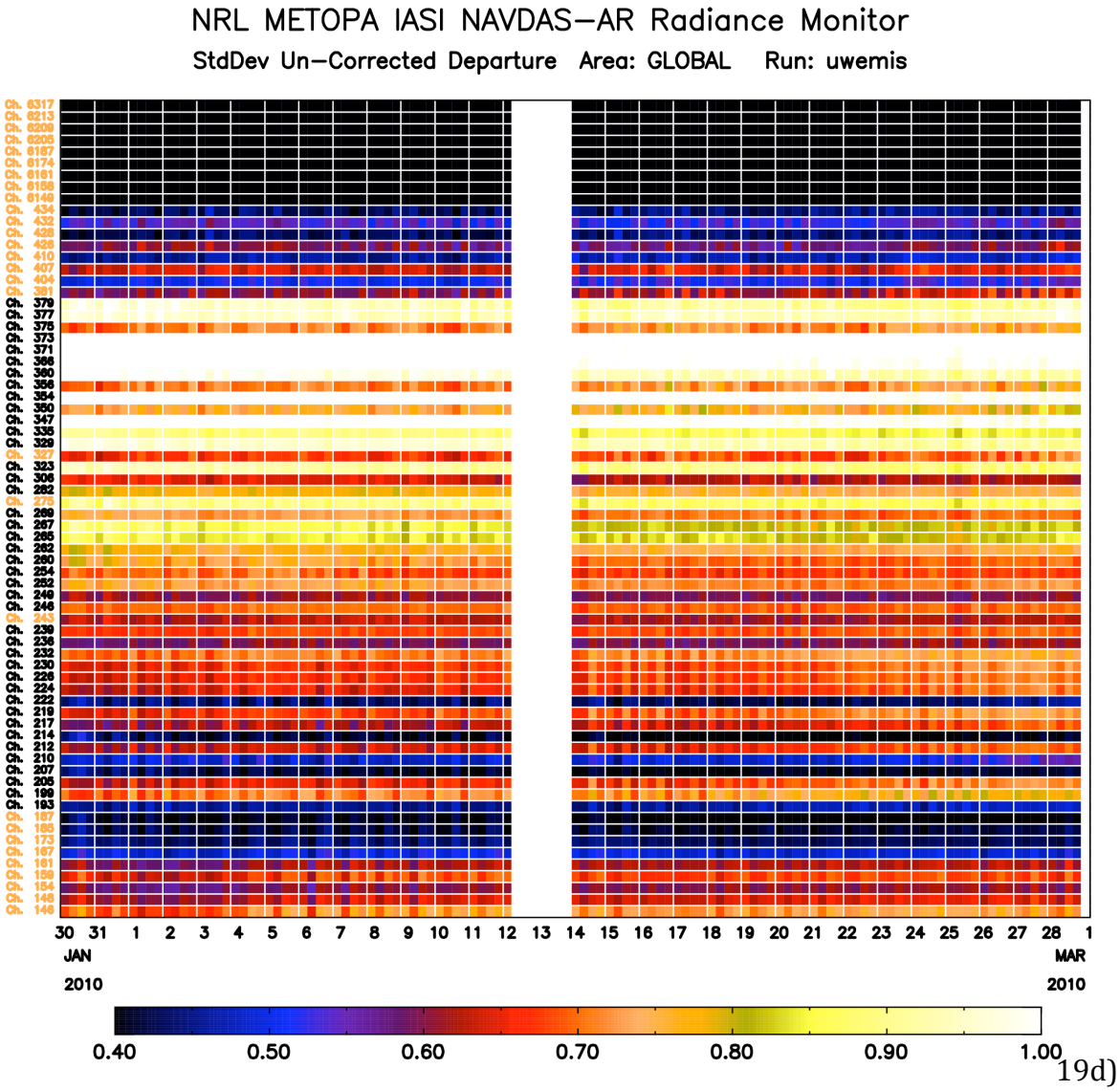

Figure 19: The global 6-hourly standard deviation of the innovations for a selection of IASI channels. Time is along the x-axis, and the IASI channels are along the y-axis with assimilated channels in black. The 'base' configuration is in panels 19a and 19c, while the 'uwemis' configuration is in panels 19b and 19d.

However, the lower tropospheric channels for the Aug2009 time period in the 'uwemis' configuration show an increase in the un-bias corrected standard deviation, which is indicative of some large innovations passing the quality control procedure. These outliers have been shown to have a detrimental effect on the forecast scores and could be the underlying reason why the positive impacts from the additional IASI radiances where not realized. Important to note is that the 'base' and 'uwemis' configurations used the same observation error over land, sea-ice and ocean. Observation errors could be inflated over both land and sea-ice to account for more of the uncertainty in these lower peaking

channels which would allow the data to still impact the analysis but with lesser weighting. It can be seen that the Feb2010 case where the standard deviations of the un-bias corrected innovations match more closely between the 'base' and 'uwemis' runs the corresponding 500hPa anomaly correlation were virtually identical. Enhancing the point that if the outliers are managed better through quality control or raised observation error than it is possible to obtain beneficial impact from these observations.

8. Conclusions and future plans

In this study, a new IR emissivity module has been developed for the RTTOV forward model to help improve estimates of the IR surface emissivity for meteorological applications, which require brightness temperature simulations, e.g. data assimilation or retrievals. First the module theory and related database were described followed by its evaluation with SEVIRI and IASI observations and its test in assimilation mode have been shown. Calculated brightness temperatures with the default RTTOV emissivity (0.98) and the new UWiremis module have been compared to the observations for four selected days representing the four seasons separately day and night. The evaluation on both the broad band SEVIRI instrument on the geostationary MSG and the high spectral resolution IASI instrument on the polar orbiting METOP-A agreed that the use of the UWiremis shows positive impact over the default value generally everywhere on the globe both day and night. The bias between the observed and calculated BT was reduced by 1.5 - 3.5 K at the 4 and 8.7 μm regions and by 0.5 – 2 K between 9.5 and 13.2 μm globally. The most significant impact occurs over very dry (sand), e.g., the Sahara region. The bias was reduced 5 - 12 K at the 4 and 8.7 μm regions. During the day the systematic bias across all surface sensitive channels can be attributed to bias error in the land surface temperature model. In addition, the error in the SW region during the day is caused by the uncertainty in the solar radiation component in the RTM. Looking at the evaluation for the four days, the biases have been significantly reduced for each time across all seasons by using the UWiremis RTTOV module. The assimilation tests were not significant at the 95% confidence level, and show that though the bias corrected innovation was spatially coherent and had a smooth transition from land to ocean, it did not correspond to an increase in forecast skill. The standard deviations of the non-bias corrected innovations show that possibly assimilating just the highest peaking channels over land is possible, and that for the mid- to lower-tropospheric channels further tuning of the observation error and revised quality control are necessary for the land and sea-ice conditions.

Certain deficiencies were identified by the research team, but overall the current version of the UWiremis module is adequate for a baseline to disseminate to the larger community where we can receive other insights and ideas for improvements. Currently the UWiremis module does not take into account any scanning angle dependence of the emissivity; we are planning to investigate and add this feature to the module in the future. The size of the error estimate array for land points may be able to be compressed by EOF analysis and will be explored as well. Lastly, the wind and temperature dependence of the ocean emissivity error estimate is not included and will be parameterized for the next version.

Acknowledgments: We would like to thank Andrew Collard and Robert Knuteson for their support and advice during this work. The laboratory data was obtained through the ASTER Spectral Library through the courtesy of the Jet Propulsion Laboratory, California

Institute of Technology, Pasadena, California. This research was supported by an Associate Scientist Mission of EUMETSAT NWP-SAF.

9. References

Borbas, E.E., R. O. Knuteson, S. W. Seemann, E. Weisz, L. Moy, and H.-L. Huang, 2007: A high spectral resolution global land surface infrared emissivity database. Joint 2007 EUMETSAT Meteorological Satellite Conference and the 15th Satellite Meteorology & Oceanography Conference of the American Meteorological Society, Amsterdam, The Netherlands, 24-28 September 2007. Available at: http://www.ssec.wisc.edu/meetings/jointsatmet2007/pdf/borbas_emissivity_database.pdf

Collard, A, 2009: Prospects for IASI, CrIS and AIRS in the UKVD, Met Office tech. Document.

Koenig, M and E de Coning (2009) The MSG Global Instability Indices Product and its Use as a Nowcasting Tool. Weather and Forecasting: 24(1) 272.

RTTOV UWIR TD, 2010: The RTTOV UWiremis IR land surface emissivity module, technical documentation by Eva Borbas, EUMETSAT, NWP-SAF, 2010.

Ruston, B.C., Weng, F. and B. Yan, 2008: Use of a One-Dimensional Variational Retrieval to Diagnose Estimates of Infrared and Microwave Surface Emissivity Over Land for ATOVS Sounding Instruments. IEEE Trans. Geosci. Remote Sens., 46, 393-402.

Salisbury, J. W. and D. M. D'Aria, 1992: Emissivity of terrestrial materials in the 8-14 µm atmospheric window. Remote Sens. Environ., 42:83–106.

Salisbury, J. W. and D. M. D'Aria, 1994: Emissivity of terrestrial materials in the 3-5 µm atmospheric window. Remote Sens. Environ., 47:345–361.

Salisbury, J. W., A. Wald, and D. M. D'Aria, 1994: Thermal-infrared remote sensing and Kirchhoff's law 1. Laboratory measurements. J. Geophys. Res., 99:11897–11911.

Seeman, S.W., Borbas, E.E., Knuteson, R.O., Stephenson, G.R. and Huang, H-L. 2008: Development of a global infrared emissivity database for application to clear sky sounding retrievals from multi-spectral satellite radiances measurements. *J. Appl. Meteorol. and Clim.* **47** *108-123.*

Wan, Z., Y. Zhang, Q. Zhang, and Z.-L. Li, 2004: Quality assessment and validation of the MODIS global land surface temperature. *Int. J. Remote Sens.*, **25**, 261-274.

Wan, Z., and Z.-L. Li, 1997: A Physics-Based Algorithm for Retrieving Land-Surface Emissivity and Temperature from EOS/MODIS Data. *IEEE Trans. Geosci. Remote Sens.*, **35**, 980-996.